Electronic supplementary information for

Rectification ratio and direction controlled by temperature in copper phthalocyanine ensemble molecular diodes

Carolina Sergi Lopes,[a] Leandro Merces,[a] Rafael Furlan de Oliveira,[a,b] Davi Henrique Starnini de Camargo,[a,c] and Carlos César Bof Bufon[a,c,d]*

[a] Brazilian Nanotechnology National Laboratory (LNNano), Brazilian Center for Research in Energy and Materials (CNPEM), 13083-970, Campinas, São Paulo, Brazil.

[b] Present address: Université de Strasbourg, CNRS, ISIS UMR 7006, 8 allée Gaspard Monge, F-67000 Strasbourg, France.

[c] Postgraduate Program in Materials Science and Technology (POSMAT), São Paulo State University (UNESP), 17033-360, Bauru, SP, Brazil.

[d] Department of Physical Chemistry, Institute of Chemistry (IQ), UNICAMP, 13084-862, Campinas, SP, Brazil.

*corresponding author: cesar.bof@lnnano.cnpem.br

Table of contents

(i) Experimental details on the EMD fabrication

The ensemble molecular diodes (EMDs) were manufactured on SiO_2-coated (2 μm thick), 9x9 mm^2 Si (100) substrates. The junction assembly relies on multiple optical lithography steps and standard microfabrication procedures, viz. thin-film deposition and controlled etching processes. All metallic layers composing the EMDs were deposited by high-vacuum (~10^{-6} Torr) e-beam evaporation (AJA International), with the substrate kept at room temperature. A Leybold Univex 250 system was employed for the evaporation of the organic materials at room temperature, in high vacuum (~10^{-5} Torr). The film thicknesses were monitored by quartz crystal microbalances placed inside the respective deposition chambers.

The EMD fabrication started with the patterning and dry reactive ion etching of a SiO_2 mesa structure on the substrate to define the bottom electrode region. Such structure was coated with a 5 nm-thick Cr adhesive layer followed by the deposition of the Au (10 nm) finger electrode. Surrounding the finger electrode, a 20 nm-thick Ge film was deposited and oxidized on a hot plate, at 60ºC for 17 h, to form a GeOx sacrificial layer. Following, Au (5 nm), Ti (10 nm), and Cr (15 nm) thin-films were sequentially deposited on top of the sacrificial layer. Such depositions were performed with evaporation rates adjusted to provide the strain gradient required for the later self-curling of the respective Au/Ti/Cr layer (roll-up technique discussed hereafter).

Prior to the so-called roll-up process, organic thin films consisting of physisorbed semiconducting molecular ensembles (SMEs) were sublimated onto the finger electrode. Precisely, *ca.* 20 nm-thick films of both copper phthalocyanine (CuPc) and its fluorinated derivative (F_{16}CuPc) were sequentially deposited onto the bottom finger electrode to compose the EMD active layers. The materials were acquired from Alfa Aesar and Sigma-Aldrich, respectively, and used without further purification. The depositions were realized individually at a rate of ~ 0.3 Å/s. Finally, the roll-up procedure was carried out in a 0.25% (v/v) H_2O_2 aqueous solution that selectively etches the GeOx sacrificial layer, leading to the NM-release from the substrate. Such a technique allows the NM strain relaxation through the spontaneous rolling-up of the Au/Ti/Cr film (Figure S1). To complete the device assembly, the rolled-up NM was architected to softly land on top of the SME-coated finger electrode,[1–5] forming Au/SMEs/Au vertical heterojunctions described here as EMDs. The NM mechanical compliance guarantees a reliable connection between the top electrode and the molecular structures,[6,7] preventing

molecules from structural damage and devices from electrical short-circuit. The as-fabricated junctions were stored in high vacuum (~10^{-5} Torr) for at least 24 h in order to remove water residues from the roll-up procedure.

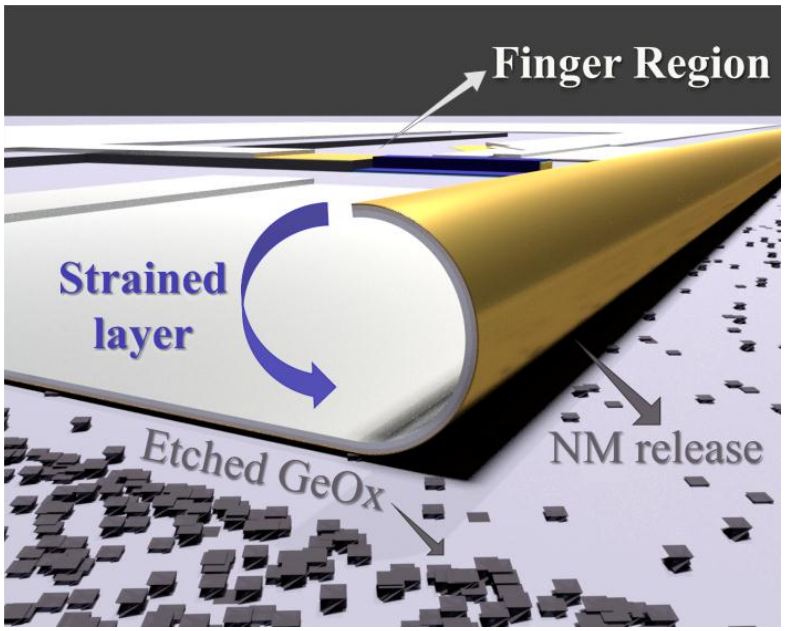

Figure S1. Schematic representation of the roll-up procedure for the formation of the EMDs.

(ii) Calculation of the activation energies

The activation energies (E_a) displayed in Table S1 and Table S2 were obtained from the Arrhenius relation described as equation S1,[8] where A is a parameter related to charge transfer rate, S is the contact area and k_B is the Boltzmann constant.

$$I \propto ASV \exp\left(\frac{-Ea}{k_B T}\right) \tag{S1}$$

Table S1 Activation energies (E_a) obtained from linear fits of the Arrhenius curves presented in Figure 3a. Three regions were chosen for the calculation of E_a, namely 20 K ≤ T ≤50 K, 70 K ≤ T ≤140 K and T > 140 K. Voltage values refer to the given I – T^{-1} traces.

	Activation energy E_a (meV)		
V^+ (V)	20 K - 50 K	70 K - 140 K	180 K - 300 K
1.6	-	-	196.29
2.2	5.34	76.47	165.52
2.8	4.79	61.24	139.60
3.4	5.34	47.59	117.23
4.0	4.22	38.60	97.21

Table S2 Activation energies (E_a) obtained from linear fits of the Arrhenius curves presented in Figure 3b. The calculation followed the same steps as in Table S1.

	Activation energy E_a (meV)		
V^- (V)	20 K - 50 K	70 K - 140 K	180 K - 300 K
1.6	-	54.43	132.38
2.2	5.18	37.29	103.30
2.8	2.90	27.07	82.39
3.4	2.35	20.18	66.19
4.0	1.77	15.23	52.05

(iii) The Au/CuPc/Au case

The absence of an abrupt organic/organic interface for Au/CuPc/Au junctions leads to no more than a moderate rectification ability. Moreover, no inversion of the rectification ratio is observed in agreement to our previous works.[1,2,8] Following, we have plotted some experimental I-V-T data acquired from measuring an Au-electrode nanomembrane-based junction having a 40 nm thick CuPc film as active material (Figure S6). One may notice that the rectification ratio RR changes from ~0.50 to ~0.06 when T decreases from 300 to 18 K (RR = $|I^-/I^+|$).

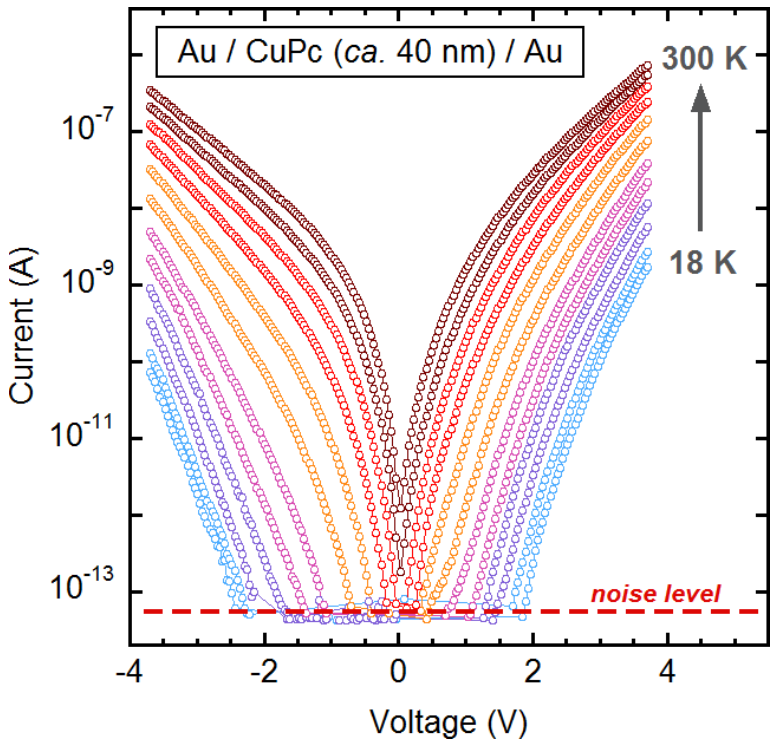

Figure S2. I-V-T data measured for Au/40 nm thick CuPc film/Au junction.

(iv) Additional current-voltage characteristics

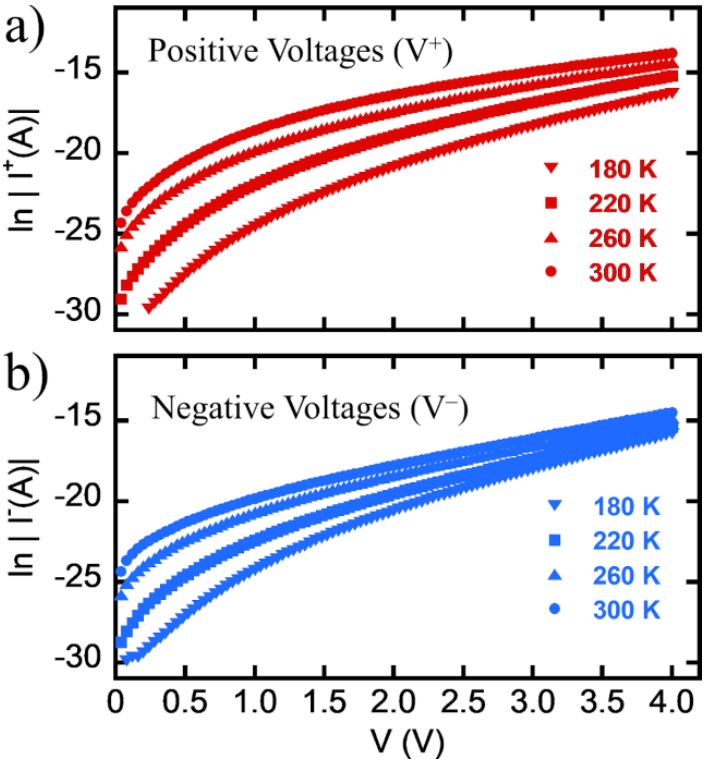

Figure S3. ln I vs V plots related to hopping conduction in the case of **(a)** positive and **(b)** negative applied voltages. Although relatively linear at |V| > 2.5 V, hopping conduction is expected to be linear mainly at low voltages.[8]

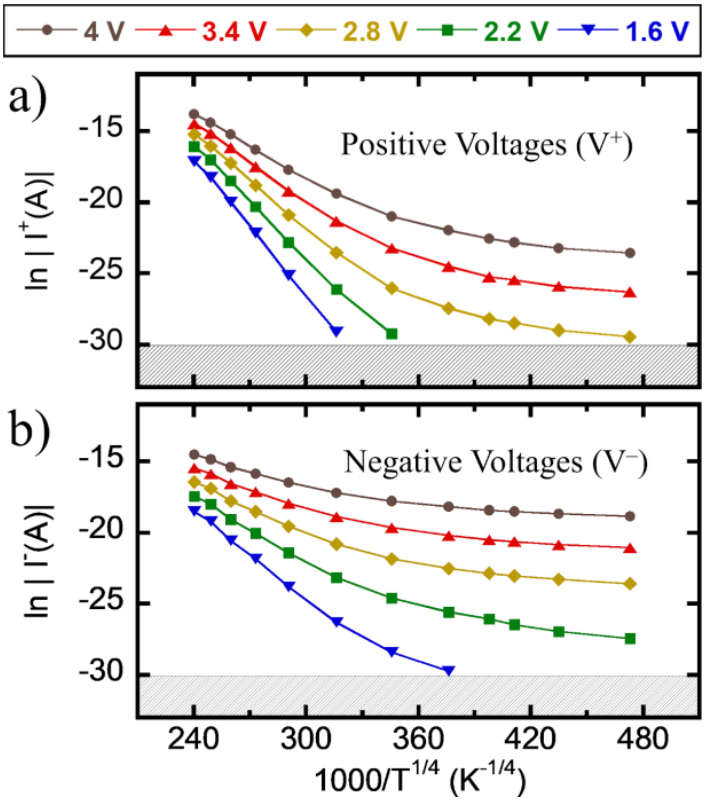

Figure S4. ln I vs. $1000/T^{1/4}$ plots related to 3D Mott variable range hopping for **(a)** positive and **(b)** negative voltages applied to the CuPc/F_{16}CuPc EMD (NM electrode biased), with temperatures ranging from 20 to 300 K.

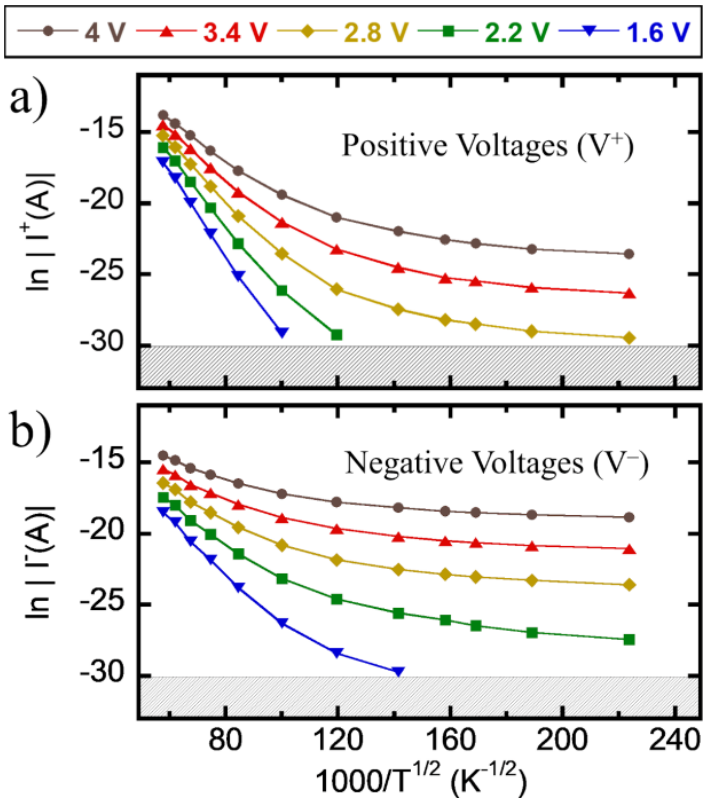

Figure S5.
ln I vs. $1000/T^{1/2}$ plots related to 1D Mott and Efros-Shklovskii variable range hopping for **(a)** positive and **(b)** negative voltages applied to the CuPc/F_{16}CuPc EMD (NM electrode biased), with temperatures ranging from 20 to 300 K.

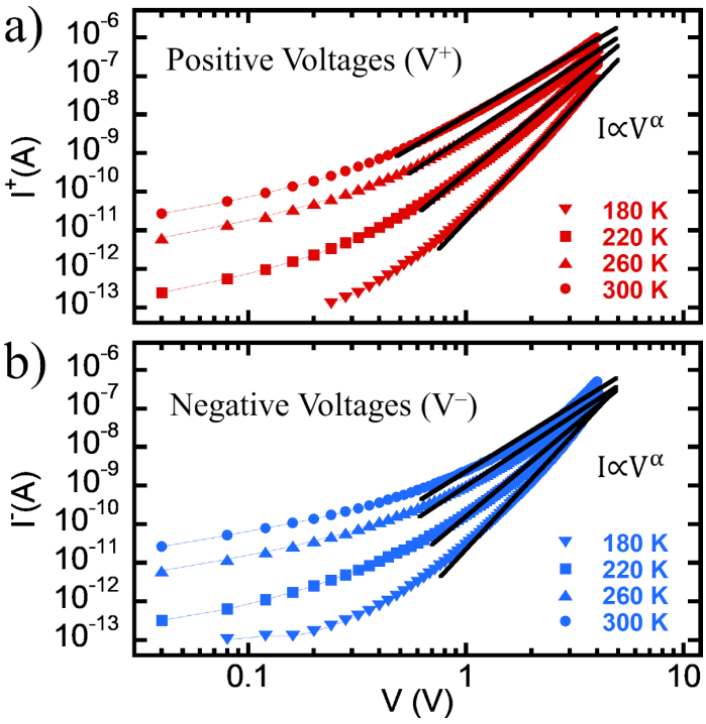

Figure S6. I vs V plots, in logarithmic scale, related to space charge limited conduction (SCLC) in the case of **(a)** positive and **(b)** negative applied voltages. By fitting a power law in the form $I \propto V^{\alpha}$, α returns values greater than 3.5. The obtained α indicates a non-conformity with SCLC.

(v) Band diagram for V=0

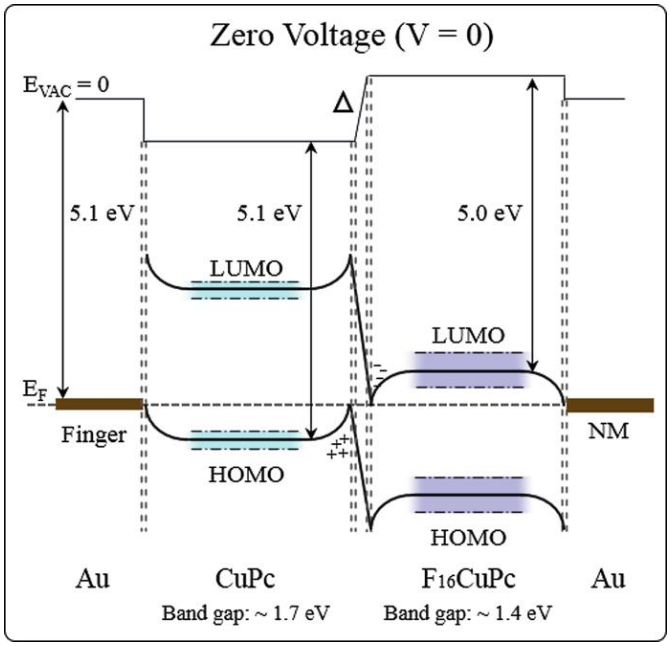

Figure S7. Band diagram for the CuPc/F_{16}CuPc EMDs at zero voltage. E_{VAC} represents the vacuum level, Δ is the vacuum level shift at the organic/organic interface and E_F is the Fermi level of the Au electrodes. Colored boxes illustrate the deviation of the mean HOMO and LUMO values found in the literature for the respective materials. This scheme is based on theoretical[9] and experimental studies.[10–13]

References

1 L. Merces, R. F. de Oliveira, D. H. S. de Camargo and C. C. B. Bufon, *J. Phys. Chem. C*, 2017, **121**, 16673–16681.
2 L.Merces, *Electronic transport in semiconducting molecular ensembles: Transporte eletrônico em conjuntos moleculares semicondutores*, Doctoral Thesis, 2018, 109, http://www.repositorio.unicamp.br/handle/REPOSIP/334402.
3 R. F. de Oliveira, L. Merces, F. Marques, É. Teixeira-Neto, D. H. S. de Camargo and C. C. B. Bufon, *J. Phys. Chem. C*, 2018, **122**, 12131–12139.
4 A. Nawaz, L. Merces, D. M. de Andrade, D. H. S. de Camargo and C. C. Bof Bufon, *Nat. Commun.*, 2020, **11**, 841.
5 G. L. Pozzoli, L. Merces, E. Yassitepe, V. B. de Morais, D. H. S. de Camargo and C. C. B. Bufon, *ACS Appl. Nano Mater.*, 2020, DOI:10.1021/acsanm.0c00523.
6 L. Merces, R. F. de Oliveira and C. C. Bof Bufon, *ACS Appl. Mater. Interfaces*, 2018, **10**, 39168–39176.
7 P. A. Petrini, R. M. Lopes da Silva, R. F. de Oliveira, L. Merces and C. C. B. Bufon, *Nanotechnology*, 2018, **29**, 265201.
8 C. C. Bof Bufon, C. Vervacke, D. J. Thurmer, M. Fronk, G. Salvan, S. Lindner, M. Knupfer, D. R. T. Zahn and O. G. Schmidt, *J. Phys. Chem. C*, 2014, **118**, 7272–7279.
9 M. Oehzelt, K. Akaike, N. Koch and G. Heimel, *Sci. Adv.*, 2015, **1**, e1501127.
10 J. Wang, H. Wang, X. Yan, H. Huang and D. Yan, *Appl. Phys. Lett.*, 2005, **87**, 093507.
11 H. Wang, J. Wang, H. Huang, X. Yan and D. Yan, *Org. Electron.*, 2006, **7**, 369–374.
12 K. M. Lau, J. X. Tang, H. Y. Sun, C. S. Lee, S. T. Lee and D. Yan, *Appl. Phys. Lett.*, 2006, **88**, 173513.
13 H. Wang and D. Yan, *NPG Asia Mater.*, 2010, **2**, 69–78.